SUPPLEMENTAL MATERIAL

Methods

Apoe$^{-/-}$*Adam15*$^{-/-}$ mice generation and animal model

A*poe*$^{-/-}$ mice (C57/BL6, Jackson Laboratory) and *Adam15*$^{-/-}$ mice (C57/BL6/129S, from Dr. Carl P. Blobel of The Hospital for Special Surgery, New York), were crossbred to generate *Apoe*$^{-/-}$ *Adam15*$^{+/-}$ mice, which were used to obtain *Apoe*$^{-/-}$*Adam15*$^{+/+}$ (n=10) and *Apoe*$^{-/-}$ *Adam15*$^{-/-}$ (n=10) littermates (Supplemental Figure 6). Atherosclerosis was induced by feeding male mice at 6 weeks of age a high-fat diet containing 1.25% cholesterol (Research Diet, New Brunswick, NJ) for 12 weeks. Then mice were sacrificed after overnight fasting. Blood was collected by heart puncture for measurement of serum lipids including triglyceride and total-, LDL- and HDL-cholesterol with kits (Bioassay Systems, Hayward, CA). To assess lesion, heart-aorta complexes were excised followed by thoracic-abdominal aortas fixed with 10% formalin while aortic sinuses and arches embedded with optimal cutting temperature (OCD) for frozen section preparation. All animal procedures were conducted in compliance with the NIH guidelines for animal research and approved by the Institutional Animal Care and Use Committee.

Oil red O staining

Oil red O staining was used to assess the size of the atherosclerotic lesion and its lipid content as previously described [1, 2]. Briefly, thoracic-abdominal aortas, cross-sections of aortic sinuses or longitudinal sections of aortic arches (6μm) were fixed with 10% formalin, dehydrated with propylene glycol and stained with 0.5% oil red O. After washing with PBS, tissue sections were counter-stained with hematoxylin (Sigma) whereas aortas were opened longitudinally and pinned on the surface of black silicon-elastomere followed by a second staining with oil red O. Zeiss

Stemi SV11 microscope with 1.0X objective was employed to observe thoracic-abdominal aortas. Zeiss Observer 200M with 10X and 20X objectives was used for aortic sinuses and arches. Digital images were obtained with the AxioVision software. For quantification, Image-Pro Plus was employed to measure the lesion size of thoracic-abdominal aortas (right after arch to the iliac bifurcation) and intimal areas of aortic sinuses (including 3 valves) and arches (3-mm segment of the lesser curvature [3]). Lipid deposition was expressed as the percentage of oil red O positive area in the intima of sinuses and arches.

Picrosirius red staining for collagen

Collagen was stained by incubating formalin-fixed frozen sections for 4 hours in 0.1% Sirius Red (Polysciences Inc., Warrington, PA) in saturated picric acid [2]. After wash with 0.01 N HCl, sections were dehydrated and mounted in Permount (Vector Laboratories). Sirius red staining was analyzed by polarizing microscopy and collagen content in intimal area of arches quantified with Image-Pro Plus.

Immunohistochemistry

Conventional avidin-biotin complex staining was employed to detect cell contents in the lesion as previously described. [1, 4] Briefly, serial frozen sections of mouse aortic arches were fixed in acetone. After inhibition of endogeneous peroxidase activity with H_2O_2 and blocking of nonspecific binding with normal rabbit serum, tissues were incubated for 90 minutes with antibodies against Mac-3 (Pharmingen, CA) and a-actin (Santa Cruz Biotech, CA) specifically for macrophages and smooth muscle cells, respectively. After washing, sections were incubated with biotinylated secondary antibody, followed by incubation with avidin–biotin–peroxidase

complex (Vector Laboratories). The chromogen 3-amino-9-ethyl carbazole (Vector Laboratories) was used as the substrate for peroxidase. After counterstaining with hematoxylin, sections were mounted with Glycerol Gelatin (Sigma). Images were obtained using Zeiss Axio Observer 200M microscope with the AxioVision software. Cell contents in the intimal lesions were determined by measuring the percentage of positive areas with Image-Pro Plus on the 3-mm segment of the lesser curvature as above [3].

Construction of ADAM15 mutant cDNA and transfection of HUVECs

Plasmid pcDNA with C-terminal hemagglutinin (HA)-tagged human wild type (WT) ADAM15 was generated as previously described [5]. A QuickChange II site-directed mutagenesis kit (Stratagene, LA Jolla, CA) was used to generate ADAM15 pcDNA mutants, including the proteolytically dead metalloproteinase by substituting alanine for the glutamate at amino acid 349 (E349A), conversion of RGD motif at 484-486 to TDD and truncation of the cytoplasmic tail at tyrosine 715 (CT) through mutation of the coding sequences corresponding to Y715 and W716 to stop codons. The primers for E349A mutation were: 5'-CCTCCATAGCCCATGCATTGGGCCACAGCCTGGGCCTG-3' (forward) and 5'-CAGGCCCAGGCTGTGGCCCAATGCATGGGCTATGGAGG-3' (reverse). For TDD mutation, the primers were: 5'-GCTGGCAGTGTCGTCCTACCACAGACGATTGTGACTTG-3' (forward) and 5'-CAAGTCACAATCGTCTGTGGTAGGACGACACTGCCAGC-3' (reverse). For CT mutation, 5'-TCCTGGTGATGCTTGGTGCCAGCTAGTGATACCGTGCC-3' and 5'-GGCACGGTATCACTAGCTGGCACCAAGCATCACCAGGA-3' were designed as forward and reverse primers, respectively. Mutations were confirmed by DNA sequencing (Davis Sequencing). For knockdown, the targeting sequences of human ADAM15 siRNA are:

5’-CCAUCUGUUCUCCUGACUU-3’, 5’-CUACCAGGCCUGAACUUCA-3’, and 5’-GACUGGCGGUGUCUUAAG-3’. Human Fyn siRNA targeting sequence was 5’-CAUCGAGCGCAUGAAUUAU-3’. Human c-Src siRNA targeting sequences were: 5’-CUCGGCUCAUUGAAGACAA-3’, 5’-UGACUGAGCUCACCACAAA-3’ and 5’-CCUCAUCAUAGCAAUAACA-3’. Human c-Yes targeting sequences were: 5’-GGAAGGAGAUGGAAAGUAU-3’, 5’-GUGACAGCAUGGUAAUGAA-3’ and 5’-CCAUGGCGUAUAUGUUCAA-3’. Human g-catenin targeting sequences were 5’-CCAGUACACGCUCAAGAAA-3’, 5’-CUCUGUGCGUCUCAACUAU-3’ and 5’-GCAUGAUUCCCAUCAAUGA-3’. All siRNA products were from Santa Cruz Biotech (Santa Cruz, CA).

For transfection, HUVEC (Combrex, MD) were maintained in endothelial growth medium (Lonza, NJ). Transient transfection of siRNA or pcDNA constructs was achieved by using Nucleofector II (Amaxa Biosystems, Cologne, Germany). All measurements were made at 72 hour post-transfection.

Primary culture of aortic endothelial cells

Primary murine aortic endothelial cells (aortic ECs) were isolated using positive immuno-selection with a rat anti-mouse CD31, as previously described [2, 6] with minor modifications. Briefly, 4-8 freshly isolated aortas were digested with 1mg/ml collagenase type I (Worthington, Lakewood, NJ) and filtered through 70μm nylon filters. Endothelial cells were purified with anti-CD31 (BD Pharmingen)-coupled magnetic beads (Invitrogen) and a magnetic separator. Primary endothelial cells were cultured in endothelial cell growth media (EGM, Lonza) and purity was >95% as examined by uptake of Dil-Ac-LDL (Biomedical Technologies, Stoughton, MA) and

flow cytometry of anti-CD31 labeling (Invitrogen). Only cells at passage 0 and 1 were used for experiments.

Albumin transendothelial flux

As an indicator of barrier properties, albumin flux across endothelial monolayers was measured as previously described [7]. Briefly, EC were grown to confluence on a transwell membrane with 0.3μm pores (Corning, NY) followed by FITC-labeled albumin (15 mM) added to the top chamber. After 2hr, concentrations of albumin in the top and bottom chambers were measured with a fluorescence microplate reader. The permeability coefficient of albumin (P_a) was determined as $P_a = [A]/t \times 1/A \times V/[L]$, where brackets denote albumin concentration in the bottom chamber [A] or the top chamber [L]; t is time (sec); A is the area of the membrane (cm^2); and V is the volume of the bottom chamber.

Monocyte isolation and transmigration

Human or murine monocytes were separated from blood by histopaque (Sigma, MO) gradient centrifugation, followed by negative selection (Stem Cell, BC, Canada), yielding a purity of 65-85% for mouse and >95% for human monocytes as examined with Gimsa-Wright's staining. For transendothelial migration, HUVECs or mouse aorta ECs were grown to confluence on 96-well transwell membranes (5μm pore size) (Millipore, CA), and 10^4 human or mouse monocytes were added to the top well, with or without 20ng/mL human (Sigma) or murine (R&D) MCP-1 in the bottom well. After 4 hours, $5X10^4$ polystyrene beads (Polysciences, PA) were added to the bottom well and transmigrated monocytes were quantified using flow cytometry, and normalized to certain number of beads.

Western blotting and Immunoprecipitation

Cells were lysed in RIPA buffer (Upsate, NY) plus phosphatase (Sigma) and protease inhibitors (Roche). Protein concentration of cell lysates was determined by BCA assay (Bio-Rad). Cell lysates corresponding to 20µg protein were fractioned by sodium dodecyl sulfate-polyacrylamide gel electrophoresis (SDS-PAGE) under reducing conditions and electrophoretically transferred to PVDF membranes (Amersham Biosciences). Membranes were blocked in 3% bovine serum albumin (BSA) in TBST (TBS with 0.1 % Tween 20), and membranes were incubated overnight at 4ºC with primary antibody, followed by 2 hours at room temperature with horseradish peroxidase (HRP)-conjugated second antibody. Membranes were developed using Pico Supersignal chemiluminescent substrate (Pierce). Stripping buffer (Thermo) was applied to the same membrane for reprobing when necessary. Films were scanned and intensity of bands quantified using NIH software Image J. For immunoprecipitation, cell lysates corresponding to 250µg protein were incubated with antibody at 4ºC for 2hr followed by overnight incubation with protein G-coupled agarose (Santa Cruz). After washing 5 times, immunoprecipitates were suspended with 1X gel loading buffer followed by SDS-PAGE and blotting as described above.

Immunofluorescence

ECs were grown to confluence in 8-well chambers (BD Falcon), fixed with 4% paraformaldehyde, permeabilized with 0.5% Saponin (Sigma) and incubated at room temperature for 1 hour with a primary antibody, followed by another 1 hour incubation with FITC-, Rhodamine- or Cy3- labeled secondary antibodies (Jackson ImmunoResearch). Cell nuclei were counterstained with Hoechst 33342 (Invitrogen). Imaging was performed using a Zeiss Axio Observer 200M inverted microscope equipped with an Apotome module (providing confocality)

and Zeiss AxioVision software.

Flow cytometry

ECs were detached with enzyme-free cell dissociation solution (Chemicon). To examine surface expression of cell adhesion molecules, *Adam15*$^{+/+}$ and *Adam15*$^{-/-}$ aortic ECs were directly stained with FITC-labeled anti-mouse PECAM-1 (Invitrogen) or VCAM-1 (BD Pharmigen), APC-labeled anti-mouse ICAM-1 (BD Pharmigen) or indirectly with a rat anti-mouse Nectin-2 antibody (Santa Cruz Biotech) followed by FITC-conjugated secondary antibody. Samples were analyzed with Accuri C6 flow cytometer equipped with CFlow Plus software. To examine the surface expression of ADAM15, cells were stained with mouse anti-ADAM15 antibody (R&D) followed by incubation with FITC-conjugated secondary antibody (Jackson ImmunoResearch). In all experiments, an identical amount of isotype IgG was applied as a control for non-specific staining.

Statistical analysis

For animal experiments, 10 *ApoE*$^{-/-}$*Adam15*$^{-/-}$ mice and 10 *ApoE*$^{-/-}$*Adam15*$^{+/+}$ littermates were involved and throughout all measurements. For *in vitro* studies, at least three completely independent experiments were performed. Data were presented as mean ± SE. Unpaired Student's t-test was employed for comparisons between two groups while one-way analysis of variance (ANOVA) with Neuman-Keuls post-hoc (Prism) was used for analyses of multiple groups. Statistical significance was defined as $p \leq 0.05$.

Reference

1. Sukhova GK, Zhang Y, Pan JH, Wada Y, Yamamoto T, Naito M, Kodama T, Tsimikas S, Witztum JL, Lu ML, Sakara Y, Chin MT, Libby P, Shi GP. Deficiency of cathepsin S reduces atherosclerosis in LDL receptor-deficient mice. *J Clin Invest.* 2003;111:897-906.

2. Sun C, Wu MH, Yuan SY. Nonmuscle Myosin Light-Chain Kinase Deficiency Attenuates Atherosclerosis in Apolipoprotein E-Deficient Mice via Reduced Endothelial Barrier Dysfunction and Monocyte Migration. *Circulation.*124:48-57.

3. Mach F, Schonbeck U, Sukhova GK, Atkinson E, Libby P. Reduction of atherosclerosis in mice by inhibition of CD40 signalling. *Nature.* 1998;394:200-203.

4. Sun C, Wu MH, Guo M, Day ML, Lee ES, Yuan SY. ADAM15 regulates endothelial permeability and neutrophil migration via Src/ERK1/2 signalling. *Cardiovasc Res.*87:348-355.

5. Najy AJ, Day KC, Day ML. The ectodomain shedding of E-cadherin by ADAM15 supports ErbB receptor activation. *J Biol Chem.* 2008;283:18393-18401.

6. Marelli-Berg FM, Peek E, Lidington EA, Stauss HJ, Lechler RI. Isolation of endothelial cells from murine tissue. *J Immunol Methods.* 2000;244:205-215.

7. Guo M, Breslin JW, Wu MH, Gottardi CJ, Yuan SY. VE-cadherin and beta-catenin binding dynamics during histamine-induced endothelial hyperpermeability. *Am J Physiol Cell Physiol.* 2008;294:C977-984.

Supplemental Table I

Supplemental Table I. Serum lipid levels in *Apoe*$^{-/-}$*Adam15*$^{+/+}$ and *Apoe*$^{-/-}$*Adam15*$^{-/-}$ mice after consumption of an atherogenic diet for 12 weeks.

Lipid (mg/dl)	*Apoe*$^{-/-}$*Adam15*$^{+/+}$ (n=10)	*Apoe*$^{-/-}$*Adam15*$^{-/-}$ (n=10)	P value*
Total Cholesterol	952.0 ± 111.1	930.3 ± 80.0	0.88
LDL	712.8 ± 58.2	719.1 ± 55.1	0.94
HDL	59.5± 5.8	53.1± 10.5	0.60
Triglyceride	81.39 ± 9.2	82.70 ± 9.0	0.92

* Unpaired Student's t-test

Supplemental Figure I

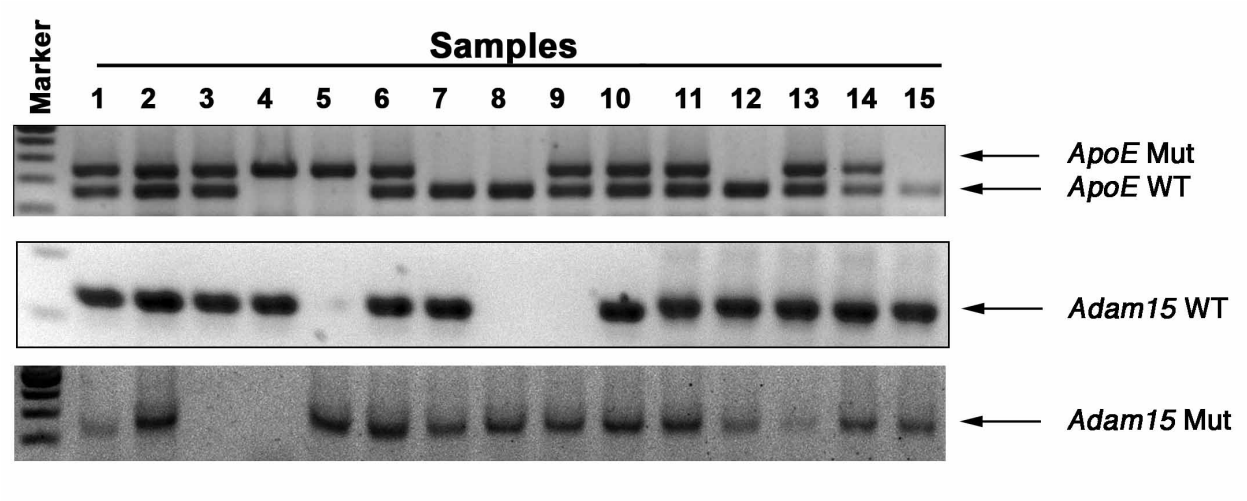

Supplemental Figure I. Generation of *Apoe*$^{-/-}$*Adam15*$^{-/-}$ mice. *Apoe*$^{-/-}$*Adam15*$^{+/+}$ and *Apoe*$^{-/-}$ *Adam15*$^{-/-}$ littermates were generated by crossbreeding *Apoe*$^{-/-}$ with *Adam15*$^{-/-}$ mice. **Top**, Representative genotyping for detecting WT or mutant (Mut) *Apoe* allele. **Middle and Bottom**, Representative genotyping for detecting WT (top) or mutant (Mut) *Adam15* allele (Bottom).

Supplemental Figure II

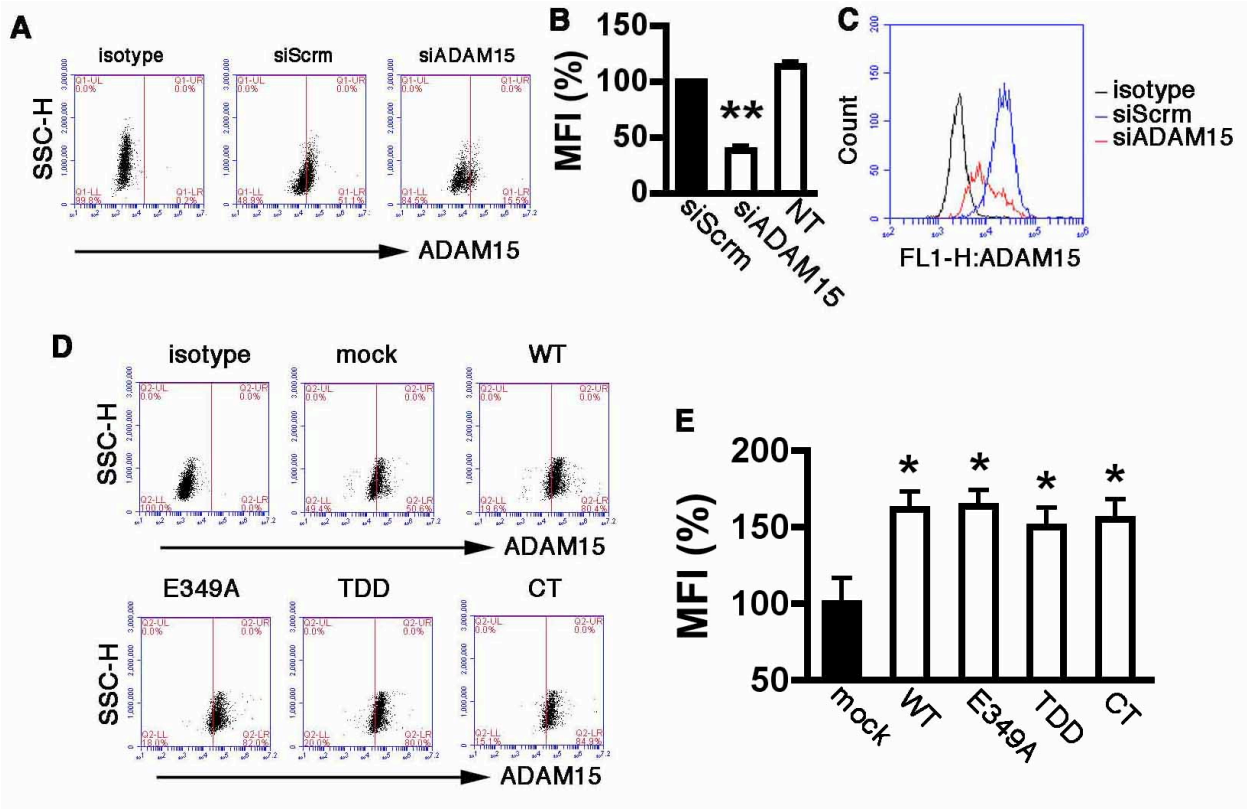

Supplemental Figure II. Knockdown and overexpression of *Adam15* on HUVEC cell surface. HUVECs were transfected with *Adam15* siRNA (**A**, **B** and **C**), WT or mutant *Adam15* cDNA (**D**, **E** and **F**) followed by flow cytometric analysis of ADAM15 expression on cell surface. **A** and **D**, representative dot plots. **B** and **E,** quantification of cell surface expression (n=5, *p<0.05, **p<0.01 vs. cells transfected with scrambled siRNA and mock). Compared with WT, neither mutation affected expression level (E, n=5) of ADAM15 on HUVEC surface. **C**, representative histograms of siRNA knockdown. NT, non-transfected.

Supplemental Figure III

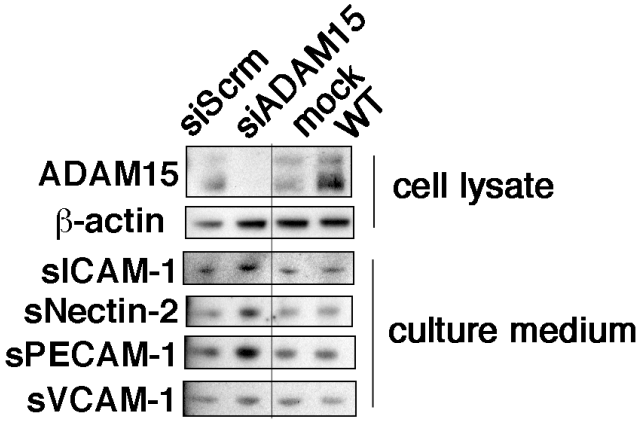

Supplemental Figure III. ADAM15 has no shedding effect on cell adhesion molecules (CAM) including ICAM-1, Nectin-2, PECAM-1 and VCAM-1. ADAM15 expression was upregulated or depleted via transfection with WT ADAM15 cDNA (WT) or ADAM15 siRNA (siADAM15) respectively. The production of soluble forms of CAMs in the medium was detected with Western blotting. Scrambled siRNA (siScrm) and empty vector (mock) served as controls respectively.

Supplemental Figure IV

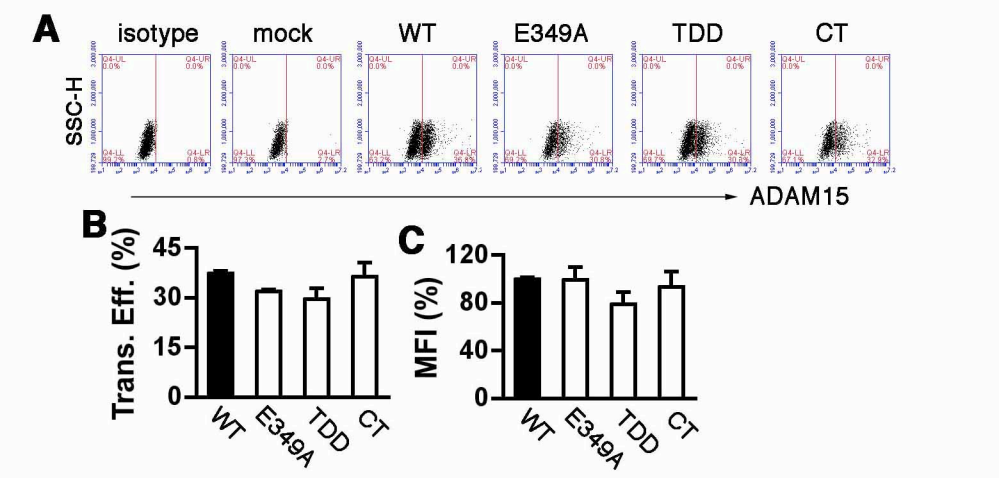

Supplemental Figure IV. Neither mutation of *Adam15* affects its rescue expression in *Adam15*$^{-/-}$ aortic ECs. *Adam15*$^{-/-}$ aortic ECs were transfected with WT or mutant *Adam15* cDNA followed by flow cytometric analysis of ADAM15 expression on cell surface. **A**, representative dot plots of flow cytometric results. **B** and **C**, neither mutation affected transfection efficiency (B, n=3) or expression level (C, n=3) of ADAM15 on aortic EC surface.

Supplemental Figure V

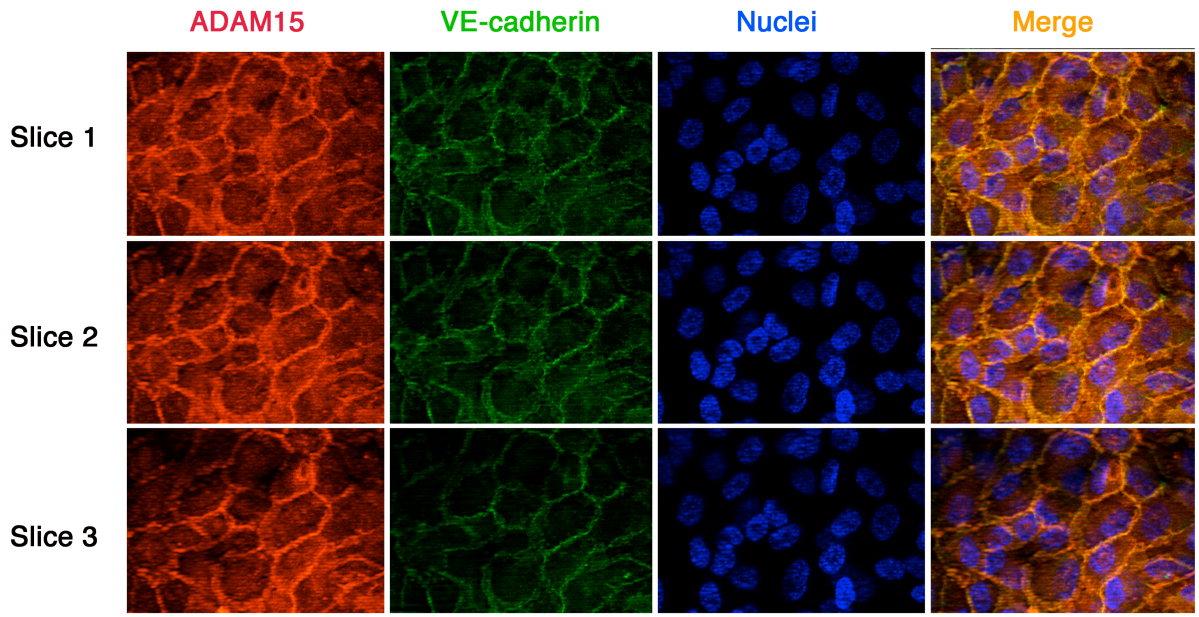

Supplemental Figure V. ADAM15 co-localizes with the adherens junction. Immunofluorescent staining demonstrated co-localization of ADAM15 (red) and VE-cadherin (green) at the cell-cell contact. Confluent HUVECs monolayers were labeled with human ADAM15 and VE-cadherin antibodies followed by Cy3- and FITC-conjugated secondary antibodies. Nuclei were counterstained with Hoechst 33342 (blue). Co-localization of ADAM15 and VE-cadherin was visible (orange or yellow) when images were merged. Imaging was performed with a Zeiss Axio Observer 200M inverted microscope equipped with an Apotome module (providing confocality) and Zeiss AxioVision software. Shown are 3 consecutive slices with a distance of 0.85μm between.

Supplemental Figure VI

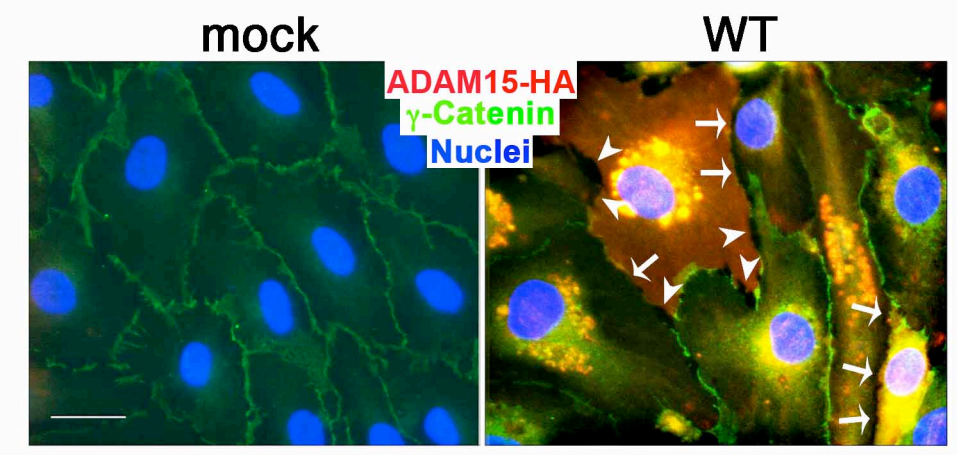

Supplemental Figure VI. ADAM15 disrupts VE-cadherin/γ-catenins association. Fluorescence immunocytochemistry in EC monolayers shows diffusion of γ-catenin at the cell periphery following overexpression of ADAM15 (right panel), compared to mock expression (left panel). Cells were stained with an anti-HA antibody (to show overexpressed ADAM15, red) and γ-catenin antibody (green). White arrows indicated areas where γ-catenin disappeared from the cell-cell contact. Arrowheads pointed to the intercellular gaps (Scale bar = 10 μm). The morphological change indicates endothelial cell-cell junction diffusion (paracellular hyperpermeability) in response to ADAM15 overexpression.

Supplemental Figure VII

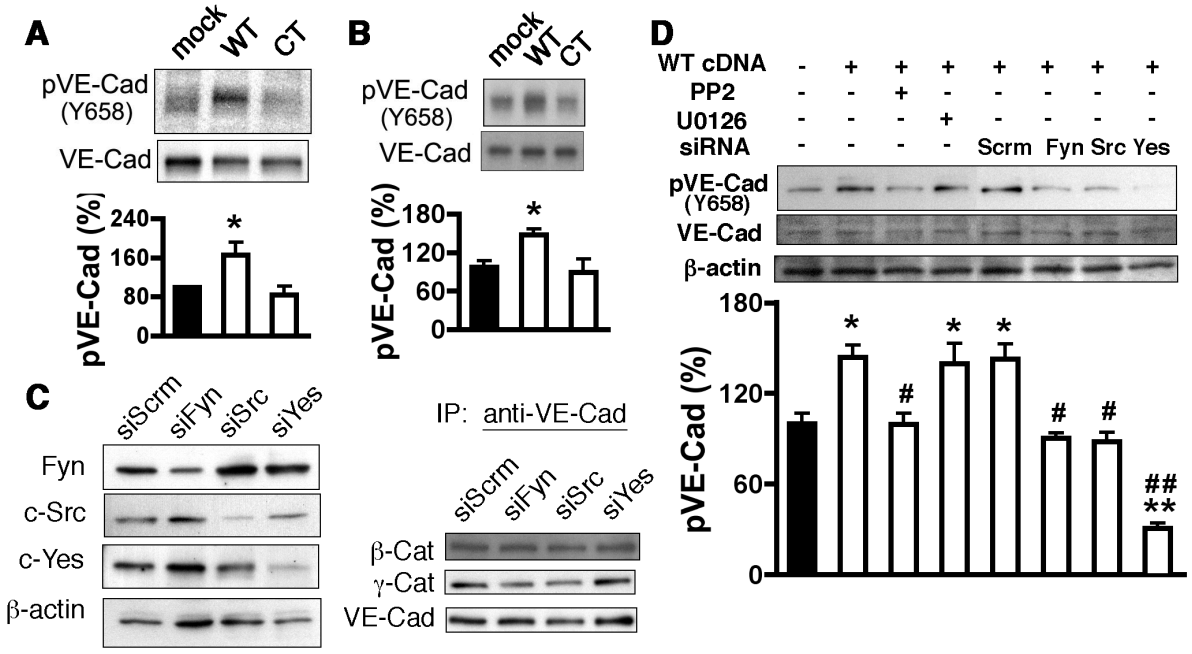

Supplemental Figure VII. Phosphorylation of VE-cadherin is concomitant with ADAM15-induced junction disassembly and can be reduced with distinct SFK knockdown. A, Transfected EC lysates were subjected to immunoblotting with a phospho-VE-cadherin (Y658)-specific antibody, and re-probed for total VE-cadherin. Overexpression of ADAM15 WT but not CT mutant in HUVECs increased VE-cadherin phosphorylation (n=3, *p<0.05 vs mock). **B**, rescue expression of WT ADAM15 in *Adam15*$^{-/-}$ mouse aortic ECs increased VE-cadherin phosphorylation (n=3, *p<0.05 vs mock). **C**, HUVECs were transfected with siRNA targeting Fyn, c-Src and c-Yes followed by assessment of VE-cadherin/catenin association with immunoprecipitation and immunoblotting. Scrambled siRNA were used as respective control. Shown are representative blots of three experiments with similar results. **D,** transfected EC were pretreated with or without 5 μmol/L PP2 or U0126 for 2 hours followed by immunoblotting with a phospho-VE-cadherin (Y658)-specific antibody, and re-probed for total VE-cadherin and β-

actin. Mock, scrambled siRNA and vehicle were used as respective control. PP2 and knockdown of each SFKs decreased VE-cadherin phosphorylation induced by ADAM15 overexpression (n=3; *$p<0.05$, **$p<0.01$ vs. cells treated with vehicle or transfected with mock; #$p<0.05$, ## $p<0.01$ vs. ADAM15 cDNA-transfected cells treated with vehicle).